Food and Energy Security
Open Access
ORIGINAL RESEARCH

Photosynthesis and growth in diverse willow genotypes

P. John Andralojc[1], Szilvia Bencze[1], Pippa J. Madgwick[1], Hélène Philippe[1], Stephen J. Powers[2], Ian Shield[3], Angela Karp[3] & Martin A. J. Parry[1]

[1]Plant Biology and Crop Science Department, Rothamsted Research, Harpenden, Hertfordshire, AL5 2JQ, United Kingdom
[2]Computational and Systems Biology Department, Rothamsted Research, Harpenden, Hertfordshire, AL5 2JQ, United Kingdom
[3]AgroEcology Department, Rothamsted Research, Harpenden, Hertfordshire, AL5 2JQ, United Kingdom

Keywords
A/Ci, carbon isotope ratio, CO_2 assimilation, photosynthesis, Rubisco, Salix

Correspondence
P. John Andralojc, Plant Biology and Crop Science Department, Rothamsted Research, Harpenden, Hertfordshire, AL5 2JQ, United Kingdom. Tel: +44 (0)1582763133;
Fax: +44 (0)1582763010;
E-mail: john.andralojc@rothamsted.ac.uk

Present address
Szilvia Bencze, Agricultural Institute, Centre for Agricultural Research, Hungarian Academy of Sciences, P.O.Box 19, Martonvásár, H-2462, Hungary

Funding Information
This work was funded by Institute Strategic Programme Grants from the Biotechnology and Biological Sciences Research Council (BBSRC; BB/J/00426X/1, BB/I002545/1, BB/I017372/1, BB/J004278/1) of the United Kingdom.

Received: 19 Feb 2014; Revised: 4 July 2014; Accepted: 15 Aug 2014

***Food and Energy Security* 2014; 3(2): 69–85**

doi: 10.1002/fes3.47

Abstract

During a study of the contribution of photosynthetic traits to biomass yield among 11 diverse species of willow, the light and CO_2 dependence of photosynthesis were found to differ, with absolute rates at ambient and saturating CO_2, together with maximum rates of Rubsico-limited and electron-transport-limited photosynthesis (V_{cmax} and J, respectively) varying by factors in excess of 2 between the extremes of performance. In spite of this, the ratio, J/V_{cmax} – indicative of the relative investment of resource into RuBP regeneration and RuBP carboxylation – was found to fall within a narrow range (1.9–2.5) for all genotypes over two successive years. Photosynthetic rate (μmol CO_2 fixed m^{-2} sec^{-1}) showed a strong, inverse correlation with total leaf area per plant. Photosynthetic capacity, expressed on a leaf area basis, showed a strong, positive correlation with yield among some of the species, but when expressed on a whole plant basis all species indicated a positive correlation with yield. Thus, both leaf area per plant and photosynthetic rate per unit leaf area contribute to this relationship. The abundance and kinetic characteristics of Rubisco play a pivotal role in determining photosynthetic rate per unit leaf area and so were determined for the chosen willow species, in parallel with Rubisco large subunit (LSU) gene sequencing. Significant differences in the rate constants for carboxylation and oxygenation as well as the affinity for CO_2 were identified, and rationalized in terms of LSU sequence polymorphism. Those LSU sequences with isoleucine instead of methionine at residue 309 had up to 29% higher carboxylase rate constants. Furthermore, the *A/Ci* curves predicted from each distinct set of Rubisco kinetic parameters under otherwise identical conditions indicated substantial differences in photosynthetic performance. Thus, genetic traits relating specifically to Rubisco and by implication to photosynthetic performance were also identified.

Introduction

Food and nonfood crops are increasingly being used as renewable sources of energy and fixed carbon for industrial processes. Such crops are the subject of intense investigation, the aim of which is to provide compelling alternatives to the use of environmentally compromising fossil fuels. Among these, short rotation coppiced (SRC) willow is finding increasing favor within temperate regions, including the United Kingdom, Northern and Eastern Europe, and North America. A recent life cycle analysis, whose objective was to identify the most resource-efficient energy crops, found that willow was second to sugar cane on the combined bases of land- and N-use efficiency (Miller 2010), making

willow among the choices of preference in regions where more tropical-adapted species, such as sugar cane, do not grow. Yields in the order of 14 tons DM ha^{-1} $year^{-1}$ have been recorded for SRC willow and are set to increase further as more productive varieties emerge (Christersson 1987; Karp et al. 2011).

All plant organic matter is derived from photosynthetic assimilation. Even so, when comparing the productivity of closely related species, leaf photosynthetic performance per se may not always be the principal cause for differences in yield. Indeed, evidence has been presented which suggests that yield and photosynthetic rate of trees may only be weakly correlated (Ericsson et al. 1996; Taylor et al. 2001). Changing requirements for development of SRC willow over the course of a single season may confine any clear correlation between photosynthetic rate and yield to periods of intense stem growth, for example, following bud burst and primary canopy establishment, typically in the late Spring/early Summer period (Cannell et al. 1987; Neergaard et al. 2002). In the field, differing degrees of competition, water stress, and pathogen interaction may also obscure any such correlation (Karp and Shield 2008).

The current research was undertaken to identify leaf characteristics which impact upon willow growth and yield. This study assessed photosynthetic capacity and contributory processes in a broad range of genotypes to determine whether sufficient natural variation relevant to yield exists to warrant the initiation of genetic improvement strategies targeting the underlying genes. The National Willow Collection at Rothamsted Research encompasses a diverse range of willow species (~100) and genotypes (~1300), exhibiting a broad range of growth habits, yield characteristics, and disease resistance traits. As such, it represents a unique resource for the identification of the genetic basis of agronomically desirable qualities, and accessions from this collection were chosen for the present study. Analyses of photosynthetic parameters of *Salix* and other woody species have been performed previously, in combination with leaf anatomical and light harvesting processes (e.g., Patton and Jones 1989; Liu et al. 2003; Robinson et al. 2004; Manter and Kerrigan 2004; Merilo et al. 2006). Similar to more recently reported work (Bouman and Sylliboy 2012), this study not only differs from these in its breadth of species diversity and range of measurements chosen but also differs from the latter work by an additional focus on the species-specific investment of resource in components of RuBP carboxylation and regeneration.

The contribution of plant leaf area to photosynthesis and yield has been extensively studied (Tharakan et al. 2005; Merilo et al. 2006; Bouman and Sylliboy 2012). The existence of two strategies among high-yielding *Salix* have been demonstrated (Tharakan et al. 2005), namely, relatively low leaf area index, but high foliar nitrogen on one hand, and high leaf area index, but low foliar nitrogen on the other, which have clear correlates in the genotypes studied here. *Salix* varieties with higher photosynthetic rates on a leaf area basis, relative to plant leaf area, have been shown to result in greater yields (Bouman and Sylliboy (2012)). Thus, in common with other commercially important plant species, improvements to photosynthetic efficiency in *Salix* has significant potential for yield improvement (Long et al. 2006).

The 11 willow accessions used in the current study included many widely used in breeding willows for bioenergy (e.g., *Salix viminalis*, *Salix eriocephala*, and *Salix schwerinii*), the parents (R13 and S3) of a key mapping population (K8) used extensively for quantitative trait locus (QTL) mapping (Hanley and Karp 2013), and a representation of diverse, pure species. Of the latter, *Salix triandra* ("Baldwin") is of particular interest as previous studies, of genetic diversity using molecular markers, have challenged the current taxonomy of this species showing it to be as distinct from most other willows species as poplar (Trybush et al. 2008). Also interesting is *Salix exigua* – a North American accession which is also distinct in terms of amplified fragment length polymorphism (AFLP) analysis and has diverse morphological traits (e.g., stomata on the upper leaf surfaces). *Salix daphnoides* was included as it is of potential interest in drought tolerance studies.

Our work aimed to determine whether a clear correlation between estimated photosynthesis and yield across a broad range of *Salix* genotypes could be demonstrated, and to identify relationships between photosynthetic capacity and the abundance of easily measured leaf components including starch, soluble carbohydrate, chlorophyll, protein, and Rubisco. The material for this study comprised pot-grown cuttings, reared under glass, during a single season of growth (2008) after which a destructive harvest took place. The rationale behind this approach was to ensure that all genotypes were subjected to identical, controlled, disease-free, growth conditions and were developmentally equivalent. This experimental approach was repeated in a second consecutive growing season (2009) in order to complement and extend the observations made in the first year. A strong correlation between Rubisco and photosynthetic performance, evident in both growing seasons, was followed up by determining the associated Rubisco large subunit (LSU) gene sequences as well as the kinetic characterization of the purified Rubisco holoenzymes, which led to the identification of three sequence polymorphisms with significant kinetic consequences.

Materials and Methods

The 11 accessions studied here are shown in Table 1 and are all present in the National Willow Collection maintained

Table 1. Identities and GenBank accession numbers of Rubisco LSU sequences.

Accession	Identity	Landrace or isolate	Abbreviation
HE610660	*Salix triandra*	Landrace Baldwin	*tri*
HE610661	*Salix dasyclados*	Isolate 77056	*das*
HE610662	*Salix udensis* (formerly *sacchalinensis*)	Landrace Sekka	*ude*
HE610663	*Salix viminalis*	Isolate bowes hybrid	*vim*
HE610664	*Salix eriocephala*	Isolate R632	*eri*
HE610665	*Salix viminalis* × *Salix schwerinii*	Isolate R13	*R13*
HE610666	*Salix viminalis* × *Salix schwerinii*	Isolate S3	*S3*
HE610667	*Salix purpurea* × *Salix viminalis*	Landrace Ulbrichtweide	*pxv*
HE610668	*Salix schwerinii*	Isolate K3 hilliers	*sch*
HE610670	*Salix daphnoides*	Isolate Fastigate	*dap*
HE610669	*Salix exigua*	–	*exi*

The abbreviations used for each genotype in subsequent figures are also shown.

at Rothamsted Research, Harpenden, UK (51°48′30″N, 0°21′22″W; 125 m AOD). The three hybrid accessions (R13, S3, and "Ulbrichtweide") are parents of mapping population families, of which R13 and S3 are full sibs of *S. viminalis* L. × *S. schwerinii* E. Wolf. All accessions are maintained as a coppiced collection and their identity has been previously verified, unless stated (Trybush et al. 2008). The pure species were chosen to represent diversity across the genus and include many that are commonly used in breeding programs worldwide.

Experimental design and growth conditions

A randomized block design with three blocks was used to conduct an experiment to assess the differences in photosynthetic performance and the yield between the 11 willow genotypes in each of two growing seasons (2008 and 2009). A set of 25–30 cm long cuttings of each genotype were collected from the National Willow Collection 1–2 months beforehand and stored in polythene bags at −4°C. In March, each was planted in a 25 cm diameter pot, containing Rothamsted prescription mix compost with added nutrients (75% medium grade [L&P] peat, 12% screened sterilized loam, 3% medium grade vermiculite, 10% grit [5-mm screened, lime free], 3.5 kg "Osmocote® Exact 3–4 month" per m^3 [Scotts (UK) Ltd., Godalming, Surrey], 0.5 kg PG mix/m^3 [Hydro Agri (UK) Ltd., Bury St. Edmunds, Suffolk], lime [approximately 3 kg/m^3 to pH 5.5–6.0], Vitax Ultrawet [wetting agent: 200 mL/m^3]) to a depth of 18–20 cm, and the design was set up in our glasshouse facilities. The pots were placed in large circular dishes which contained water at all times, to avoid drought stress. Supplementary lighting was provided to ensure an irradiance of at least 400 μmol m^{-2} sec^{-1} throughout the light period (16 h day/8 h night). Bud emergence did not take place until April. The experiment was terminated by shoot harvest in late December.

Leaf gas exchange measurements

Light and CO_2 dependence of photosynthesis was measured for all genotypes in 2008 and 2009. Leaf photosynthesis was measured at midday ±3 h, on young, fully expanded leaves attached to the dominant stem of each plant, using a gas exchange analyzer equipped with an LED light source (Li-6400, Li-Cor Inc., Lincoln, Nebraska, USA). Instrument start-up/calibration according to the manufacturer's instructions was performed at the start of each day. Leaf chamber conditions, unless stated otherwise, consisted of a photosynthetic photon flux density of 1250 μmol photons m^{-2} sec^{-1} (with 10% blue light) and a CO_2 concentration of 385 μmol mol^{-1}. During measurement, leaf temperature was maintained at 25 ± 1.5°C and relative humidity at 60%. For *A*/*Ci* curves, reference CO_2 values of 450, 300, 150, 75, 450, 600, 800, and 1100 μmol mol^{-1} were applied. For *A*/*Q* curves, the sample CO_2 concentration was set to 385 μmol mol^{-1} and photosynthesis measured at light levels of 1500, 1000, 750, 500, 250, 125, 50, and 0 μmol photons m^{-2} sec^{-1}. Each data point was logged when the change in each of CO2S, H2OS, Flow, Photo, and Cond were no more than 1% CV (coefficient of variation) over a 20-sec period. At low deltas (<15 ppm CO_2), the IRGAS were matched immediately before measurement. The resulting *A*/*Ci* data were processed using a published algorithm (Sharkey et al. 2007) to determine values – normalized to the reference temperature of 25°C – of the maximum carboxylation rate allowed by Rubisco, V_{cmax} (i.e., the product of Rubisco carboxylase activity and Rubisco abundance per unit leaf area), and the rate of photosynthetic electron transport, *J* (based on NADPH requirement), while also providing estimates for day respiration and mesophyll conductance. To increase accuracy, values for the relevant Rubisco kinetic parameters used by this algorithm (the K_M for carboxylase [K_c] and oxygenase [K_o] activities and the specificity factor [$S_{c/o}$]), were determined using Rubisco purified from the genotypes under study.

The gas exchange data describing the light dependence of photosynthesis were used to determine the light-saturated rate of photosynthesis (A_{maxQ}), the irradiance required to achieve half this value ($Q_{½}$), and the light compensation

point (Γ_Q). This was made possible, since the (A/Q) paired data points were faithfully described by the function:

$$A = A_{maxQ}(Q-\Gamma_Q)/[Q_{1/2}+(Q-\Gamma_Q)], \quad (1)$$

where A is the observed rate of CO_2 assimilation at light intensity Q. An Excel solver routine was constructed to find the best fit of the experimental data to this equation, by varying the values of A_{maxQ}, $Q_{½}$, and Γ_Q.

Measurement of growth and leaf area per plant

The number, length, and diameter (at 0.5-m intervals) of all shoots and branches were systematically tabulated, together with the number and area of all the associated leaves. Leaf area was measured using a Li-Cor LI-3000 leaf area meter, which enabled the rapid and nondestructive measurement of leaf area, length, and width. It took approximately 10 days to process all 33 samples (11 × 3 replicates) and this task was performed on two separate occasions: from mid-June and from early August (2009). As soon as this task had been completed, the associated gas exchange measurements were made.

Leaf sampling and extraction for quantification of starch, chlorophyll, soluble protein, and Rubisco

Leaf samples (10 cm^2) taken in the early Summer, 3–4 h after midday, were snap-frozen in liquid N_2 immediately after excision from the plant by means of a 3.6 cm diameter cork borer and stored at −80°C until extraction. Extraction buffer consisted of: 50 mmol/L MES-NaOH, pH 7.0; 10 mmol/L $MgCl_2$; 1 mmol/L ethylene glycol tetraacetic acid (EGTA); 1 mmol/L ethylenediamine-tetraacetic acid (EDTA); 50 mmol/L 2-mercaptoethanol; 1% (v/v) Tween 80; 2 mmol/L benzamidine; 5 mmol/L ε-aminocaproic acid; 10 mmol/L D,L-dithiothreitol; 1% (v/v) Sigma plant protease inhibitor cocktail (P 9599); and 1 mmol/L PMSF – the last three components being added immediately before extraction. Three milliliters of this buffer was used per 10 cm^2 of leaf material, as follows: 0.5 mL of extraction buffer was first ground to a fine powder in liquid N_2 by means of a precooled pestle and mortar. To this was added the frozen leaf tissue together with 0.2 g acid washed sand, which were ground to a fine powder. A further 0.5 mL of extraction buffer was added and ground-in, followed by two more aliquots of 1 mL with accompanying grinding. The homogeneous paste was allowed to thaw, accompanied by frequent grinding. Once thawed, a 0.70 mL subsample was taken for immediate chlorophyll and starch determination, and the remaining homogenate was clarified by centrifugation (5 min, 4°C, 14,250 × g). The clarified supernatant was divided into 0.40 mL aliquots and snap-frozen until needed. This procedure releases large quantities of soluble protein which (in the case of Rubisco) retains full catalytic activity and can be scaled-up, as necessary, for the purification of sufficient Rubisco for specificity factor assays. To determine the soluble protein in these Tween-containing samples, we found the 2-D Quant Kit (GE Healthcare, Hatfield, Hertfordshire, UK) to be ideal, on account of its sensitivity and the incorporation of an acid-precipitation step, enabling removal of interfering solutes (including Tween 80) prior to protein-dependent color development. The homogenized samples taken prior to centrifugation for chlorophyll and starch determination were added immediately to ethanol (giving 90% [v/v] ethanol) and the chlorophyll content of the clarified solution determined spectrophotometrically as described by Wintermans and De Mots (1965). The resulting insoluble, decolorized pellet could then be assayed sequentially for soluble carbohydrate then starch content, using anthrone – a reagent specific for soluble carbohydrate – by a modification of the approach of Hansen and Møller (1975) in which the soluble carbohydrate was first removed from the insoluble starch by repeated extraction/sedimentation first using 80% (v/v) and then 50% (v/v) ethanol. The sugar content of the combined ethanolic supernatants was then determined, while the resulting starch-containing pellet was dried under vacuum, and starch digestion initiated by addition of 0.5 mL of 100 mmol/L sodium acetate (pH 4.5) containing 10 units mL^{-1} of purified amyloglucosidase (Product A 7420, Sigma Aldrich Co Ltd., Poole, Dorset, UK). Digestion proceeded at 37°C for 24 h, after which the digests were clarified by centrifugation and the sugar content determined by the anthrone method. A parallel digestion control was always performed, to enable correction for traces of soluble carbohydrate present in the amyloglucosidase itself.

Rubisco extraction for kinetic assays

This was achieved by a small-scale extraction procedure very similar to that described earlier, except that by the time these were performed it had been found that excellent Rubisco activities could also be obtained by replacing Tween 80 with PEG 4000. An important consequence of this (the absence of Tween 80) was that the Rubisco could then be quantified by the quicker ^{14}CABP-binding method of Yokota and Canvin (1985) rather than by band quantification following SDS-PAGE. Leaf material for this purpose was from youngest, fully expanded leaves, sampled in late Spring/early Summer (2008) and mid/late Summer (2009). The complete extraction buffer for this purpose was: 50 mmol/L MES-NaOH, pH 7.0; 5 mmol/L $MgCl_2$; 1 mmol/L EGTA; 1 mmol/L EDTA; 50 mmol/L 2-mercaptoethanol; 10 mmol/L $NaHCO_3$; 2 mmol/L benzamidine; 5 mmol/L ε-aminocaproic acid; 5% (w/v) PEG 4000; 10 mmol/L D,L-dithiothreitol; 1% (v/v) Sigma plant protease inhibitor cocktail (P 9599); insoluble

PVPP (150 mg gFW^{-1}), and 1 mmol/L PMSF – the last four ingredients being added immediately before extraction. The resulting, clarified supernatant was then immediately applied to a PD-10 desalting column (GE Healthcare) at 4°C, pre-equilibrated, and subsequently developed with the following ice-cold buffer: 100 mmol/L Bicine-NaOH, pH 8.2; 10 mmol/L $MgCl_2$; 1 mmol/L EDTA; 1 mmol/L benzamidine; 1 mmol/L ε-aminocaproic acid; 1 mmol/L Na_2HP_i; 10 mmol/L $NaHCO_3$; 2% (w/v) PEG 4000; 10 mmol/L D,L-dithiothreitol. Fractions of 0.5 mL were collected and two or three fractions containing the protein peak were pooled, supplemented with 1% (v/v) Sigma plant protease inhibitor cocktail (P 9599) and snap-frozen in liquid N_2, and stored in liquid N_2 until assayed. Pilot experiments established that freezing in this way had no effect on subsequent catalytic activity.

Rubisco kinetic characterization

Rates of Rubisco $^{14}CO_2$-fixation using rapidly extracted and desalted leaf protein extracts were measured in 7 mL septum-capped scintillation vials, containing reaction buffer (yielding final concentrations of 100 mmol/L Bicine-NaOH, pH 8.0, 20 mmol/L $MgCl_2$, 0.4 mmol/L RuBP, and about 100 W-A units of carbonic anhydrase) and sodium [^{14}C] bicarbonate to give one of six different concentrations of CO_2 (4–100 μmol/L, each with a specific radioactivity of 3.7×10^{10} Bq mol^{-1}), each at four concentrations of O_2 (0%, 21%, 60%, and 100% [v/v]), as described previously (Parry et al. 2007). Assays (1.0 mL total volume) were started by the addition of activated leaf extract, and the V_{max} for carboxylase activity, together with the Michaelis–Menten constant (K_m) for CO_2 (K_c) determined by application of a curve optimization program (Enzfitter, Elsevier Biosoft, PO Box 98, Cambridge, UK). The K_m for the oxygenase activity (K_o) was calculated from the relationship, $K_{c,(21,61,100\%o_2)} = K_{c,(0\%O_2)}(1+[O_2]/K_o)$ using the corresponding apparent K_c values at 21%, 60%, and 100% O_2. Replicate measurements (n = 2–8) were made using protein preparations from leaves of different individuals. For each sample, the maximum rate of carboxylation (k^c_{cat}) was extrapolated from the corresponding V_{max} value after allowance was made for the Rubisco active site concentration, as determined by [^{14}C]CABP binding (Yokota and Canvin 1985). Rubisco CO_2/O_2 specificity ($S_{c/o}$) was measured as described (Galmés et al. 2005) using enzyme purified by PEG precipitation and ion-exchange chromatography and the values given for each species were the mean of 5–6 replicate determinations. The maximum oxygenation rate (k^o_{cat}) was calculated using the equation $S_{c/o} = (k^c_{cat}/K_c)/(k^o_{cat}/K_o)$. All kinetic measurements were performed at 25°C. All radiochemicals and associated instruments and consumables were purchased from PerkinElmer (Seer Green, Buckinghamshire, UK). All other chemicals were of analytical grade and supplied by Sigma.

As described in the Discussion section, the maximum carboxylation rate of Rubisco (V_{cmax}) for each willow species could be calculated after determination of the leaf Rubisco concentration and the corresponding rate constant for carboxylation, using the equation:

$$V_{cmax} = \text{Rubisco concentration } (g \cdot m^{-2}) \times k^c_{cat}(s^{-1}) \times 14.5 \mu\text{mol active sites} \cdot \text{g Rubisco}^{-1}, \quad (2)$$

(assuming a molecular weight (MW) of 550 kDa for Rubisco and eight active sites per Rubisco holoenzyme). [Correction added on 15 December 2014 after initial publication on 10 October 2014. In Equation 2, the final term Rubisco^{-1} should be g Rubisco^{-1}. This is now corrected.]

Biomass measurement and yield estimation

The number, length, and diameter (at 0.5 m intervals) of all shoots and branches were systematically tabulated immediately prior to harvest. Aboveground material from each sample, excluding any remaining leaves, was cut into 25 cm lengths, weighed, then oven dried at 80°C for 96 h, and reweighed immediately. The resulting dry mass (DM) data are regarded as the biomass yield. A nondestructive estimate of yield in early and again in mid/late Summer (2009) was provided by measurement of shoot and branch numbers, length, and diameters at 0.5 m intervals, from which the total shoot volume could be calculated, which was highly correlated to wood DM (Table 3, col 1, row A).

LSU gene sequencing

DNA was extracted from two young leaves of each willow variety, by use of the Wizard™ Genomic DNA Isolation Kit (Product A1120, Promega, Southampton, UK). These preparations included chloroplast DNA. *rbcL* was amplified from primers binding within the genes on either side of *rbcL* in the chloroplast genome, ATP synthase β (atpB3: GTGTCAATC ACTTCCATTCCTCTC), and acetyl-CoA carboxylase β (accDR2: CCATTGATTTAYTTCRCCYACACCTG). DNA sequencing of purified PCR products was carried out from these primers and additional primers SF1, SF2, SR1, and SR2 (CGAGTAGACCTTGTTGCTGTGAG; CTTCTACTGGTACA TGGACAACTG; CTTTTAGTAAAAGATTGTTCCTAT; CAT CTTTGGTAAAATCAAGTCCACC).

Statistical analysis

Association between mean values (three biological replications per genotype) of the indicated genotype-specific parameters (11 genotypes per parameter set) were calculated using the Pearson product–moment correlation (Tables 2, 3), as implemented by SigmaPlot 12.0 (Systat Software, Inc., Hounslow, London, UK) highlighting correlation coefficients

Table 2. Pearson product–moment correlations between mean values for a variety of yield- and photosynthesis-related parameters, determined for each genotype in 2008.

Leaf size	SLA	Leaf area	A_{amb}	*Ci*	ΣA_{amb}	A_{max}	V_{cmax}	Rubisco	*J*	$Q_{½}$	A_{maxQ}	Γ_Q	*CHO*	Starch	*Chl*	a/b	Protein			
1	2	3	4	5	6	8	9	10	11	12	13	14	15	16	17	18	19			
0.36	0.57	0.61	−0.48	0.45	0.71	−0.64	−0.67	−0.66	−0.62	−0.66	−0.77	−0.46	0.22	0.55	−0.31	0.47	−0.59	A	Shoot DM	g/plant
	0.12	0.65	−0.86	−0.16	0.53	−0.68	−0.69	−0.65	−0.70	−0.84	−0.77	−0.34	0.61	0.52	−0.41	0.66	−0.71	B	Leaf size	cm^2/leaf
		0.12	−0.09	0.19	0.16	−0.19	−0.21	−0.20	−0.22	−0.41	−0.47	−0.72	−0.10	0.15	−0.19	0.53	−0.27	C	SLA	cm^2/g
			−0.75	−0.15	0.96	−0.72	−0.67	−0.67	−0.71	−0.85	−0.88	−0.52	0.63	0.75	−0.30	0.39	−0.90	D	Leaf area	m^2/plant
				0.07	−0.63	0.77	0.77	0.71	0.78	0.81	0.80	0.30	−0.51	−0.71	0.61	−0.77	0.73	E	A_{amb}	μmol m^{-2} sec^{-1}
					−0.08	−0.32	−0.40	−0.28	−0.31	0.18	0.00	−0.20	−0.51	0.22	−0.38	0.12	0.06	F	*Ci*	μmol mol^{-1}
						−0.65	−0.61	−0.67	−0.63	−0.81	−0.86	−0.48	0.66	0.65	−0.20	0.27	−0.83	G	ΣA_{amb}	μmol/m^2/plant
							0.98	0.95	1.00	0.73	0.83	0.47	−0.33	−0.89	0.68	−0.53	0.85	I	A_{max}	μmol/m^2/sec
								0.94	0.98	0.68	0.79	0.39	−0.27	−0.81	0.72	−0.57	0.78	J	V_{cmax}	μmol/m^2/sec
									0.95	0.76	0.86	0.40	−0.47	−0.79	0.67	−0.45	0.80	K	Rubisco	g/m^2
										0.73	0.83	0.51	−0.34	−0.90	0.70	−0.58	0.86	L	*J*	μmol/m^2/sec
											0.97	0.43	−0.80	−0.69	0.28	−0.65	0.86	M	$Q_{½}$	μmol/m^2/sec
												0.52	−0.73	−0.78	0.38	−0.68	0.91	N	A_{maxQ}	μmol/m^2/sec
													−0.30	−0.61	0.15	−0.56	0.70	O	Γ_Q	μmol/m^2/sec
														0.29	0.08	0.22	−0.60	P	*CHO*	g/m^2
															−0.60	0.47	−0.84	Q	Starch	g/m^2
																−0.49	0.36	R	Chl	g/m^2
																	−0.50	S	a/b	

Each measurement was the mean of three biological replications. $P < 0.05$ ($r = 0.60 – 0.72$) is indicated by a yellow background and $P < 0.01$ ($r = 0.73+$) by green. A_{amb}, photosynthesis at ambient CO_2 with 1250 μmol PAR m^{-2} sec^{-1}, 25°C, 60% relative humidity. *A,* net rate of CO_2 uptake per unit leaf area (μmol m^{-2} sec^{-1}); A_{amb}, A_{max}, *A* as measured in air containing ambient (385 μmol mol^{-1}) or saturating (1100 μmol mol^{-1}) concentrations of CO_2, respectively; A_{maxQ}, theoretical value of *A* prevailing at light saturation; *Ci,* intercellular CO_2 concentration (μmol mol^{-1} at ambient external CO2); $Q_{½}$, irradiance at which ½ A_{maxQ} is attained (μmol photons m^{-2} sec^{-1}); ΣA_{amb}, net rate of CO_2 uptake per plant (μmol m^{-2} $plant^{-1}$); Γ_Q, light compensation point (μmol photons m^{-2} sec^{-1}); V_{cmax}, maximum rate of RuBP carboxylation (μmol CO_2 fixed m^{-2} sec^{-1}); *J*, rate of whole chain electron transport (μmol electrons m^{-2} sec^{-1}); SLA, specific leaf area (cm^2 g^{-1}); *CHO*, soluble carbohydrate (g m^{-2}); *Chl*, total chlorophyll concentration (g m^{-2}); *a/b*, ratio of Chl a: Chl b (dimensionless); *protein*, total soluble leaf protein (g m^{-2}).

Table 3. Pearson product–moment correlations between mean values for a variety of yield- and photosynthesis-related parameters, determined for each genotype in 2009.

At harvest		Early Summer													Mid/late Summer							
Shoot V	Root DM	Leaf size	A_{amb}	$A_{amb}M$	*Ci*	A_{max}	V_{cmax}	*J*	$Q_{½}$	A_{maxQ}	Γ_Q	Shoot *V*	Leaf area	ΣA_{amb}	Shoot *V*	Leaf area	Rubisco	A_{amb}	ΣA_{amb}			
1	2	3	4	5	6	7	8	9	10	11	12	13	14	15	16	17	18	19	20			
0.97	0.88	0.34	−0.40	−0.46	−0.07	−0.28	−0.45	−0.26	−0.69	−0.61	−0.32	0.63	0.73	0.87	0.88	0.48	−0.26	−0.53	0.38	A	Shoot DM	g/plant
	0.88	0.36	−0.37	−0.40	−0.13	−0.19	−0.34	−0.17	−0.61	−0.57	−0.33	0.68	0.71	0.88	0.94	0.35	−0.13	−0.49	0.28	B	Shoot V	cm^3 $plant^{-1}$
		0.40	−0.49	−0.53	−0.06	−0.40	−0.51	−0.40	−0.69	−0.69	−0.28	0.43	0.76	0.90	0.72	0.54	−0.38	−0.44	0.49	C	Root DM	g/plant
			−0.68	−0.57	−0.05	−0.69	−0.54	−0.69	−0.64	−0.66	−0.29	0.33	0.63	0.42	0.38	0.50	−0.44	−0.48	0.19	D	Leaf size	cm^2/leaf
				0.90	0.42	0.81	0.80	0.82	0.64	0.96	0.57	−0.50	−0.89	−0.68	−0.37	−0.78	0.61	0.68	−0.27	E	A_{amb}	µmol m^{-2} sec^{-1}
					0.25	0.89	0.87	0.88	0.62	0.86	0.36	−0.27	−0.86	−0.69	−0.30	−0.82	0.77	0.60	−0.45	F	$A_{amb}M$	µmol m^{-2} sec^{-1}
						−0.05	0.16	0.00	−0.25	0.35	0.65	−0.40	−0.40	−0.37	−0.33	−0.15	−0.28	0.49	0.41	G	*Ci*	µmol mol^{-1}
							0.81	0.95	0.69	0.77	0.10	−0.07	−0.66	−0.43	−0.05	−0.81	0.88	0.49	−0.49	H	A_{max}	µmol m^{-2} sec^{-1}
								0.91	0.58	0.77	0.48	−0.12	−0.73	−0.56	−0.23	−0.82	0.81	0.59	−0.54	I	V_{cmax}	µmol m^{-2} sec^{-1}
									0.61	0.75	0.27	−0.03	−0.67	−0.43	−0.06	−0.88	0.91	0.52	−0.48	J	*J*	µmol m^{-2} sec^{-1}
										0.77	0.20	−0.48	−0.68	−0.62	−0.47	−0.58	0.60	0.33	−0.62	K	$Q_{½}$	µmol m^{-2} sec^{-1}
											0.51	−0.58	−0.93	−0.81	−0.52	−0.79	0.58	0.69	−0.37	L	A_{maxQ}	µmol m^{-2} sec^{-1}
												−0.55	−0.56	−0.48	−0.51	−0.39	0.07	0.47	0.14	M	Γ_Q	µmol m^{-2} sec^{-1}
													0.60	0.63	0.83	0.20	0.09	−0.59	−0.20	N	Shoot V	cm^3 $plant^{-1}$
														0.93	0.67	0.69	−0.49	−0.64	0.35	O	Leaf area	m^2 $plant^{-1}$
															0.81	0.57	−0.32	−0.59	0.34	P	ΣA_{amb}	µmol m^{-2} $plant^{-1}$
																0.26	0.05	−0.59	−0.02	Q	Shoot *V*	cm^3 $plant^{-1}$
																	−0.84	−0.75	0.41	R	Leaf area	m^2 $plant^{-1}$
																		0.40	−0.53	S	*Rubisco*	g m^{-2}
																			0.17	T	A_{amb}	µmol m^{-2} sec^{-1}

Each measurement was the mean of three biological replications. $P < 0.05$ ($r = 0.61 – 0.70$) is indicated by a yellow background and $P < 0.01$ ($r = 0.71+$) by green. *A*, net rate of CO_2 uptake per unit leaf area (µmol m^{-2} sec^{-1}); A_{amb}, A_{max}, *A* as measured in air containing ambient (385 µmol mol^{-1}) or saturating (1100 µmol mol^{-1}) concentrations of CO_2, respectively; $A_{amb}M$, A_{amb} derived by biochemical modelling; A_{maxQ}, theoretical value of *A* prevailing at light saturation; *Ci*, intercellular CO_2 concentration (µmol mol^{-1}) at ambient external CO2; $Q_{½}$, irradiance at which ½ A_{maxQ} is attained (µmol photons m^{-2} sec^{-1}); ΣA_{amb}, net rate of CO_2 uptake per plant (µmol m^{-2} $plant^{-1}$); Γ_Q, light compensation point (µmol photons m^{-2} sec^{-1}); V_{cmax}, maximum rate of RuBP carboxylation (µmol CO_2 fixed m^{-2} sec^{-1}); *J*, rate of whole chain electron transport (µmol electrons m^{-2} sec^{-1}); SLA, specific leaf area (cm^2 g^{-1}); V, volume (cm^3 $plant^{-1}$); DM, dry mass (g $plant^{-1}$).

Table 4. Comparing Rubisco from the chosen *Salix* genotypes.

Species	Polymorphic residues						Rubisco kinetic constants									
Spinach	9	142	230	255	309	363	k^c_{cat} (sec^{-1})		k^o_{cat} (sec^{-1})		K_c(μM)		K_o(μM)		$S_{c/o}$	
	A	V	A	V	M	Y	Mean	LSD	Mean	LSD	Mean	LSD	Mean	LSD	Mean	LSD
S. triandra	A	P	T	I	I	Y	3.45	0.35	2.24	0.54	7.2	1.46	409	104	88.3	3.1
R13	T	T	A	I	I	Y	2.78		1.17		11.0		408		88.4	
S. exigua	T	V	A	V	M	F	2.67		1.78		6.4		379		88.5	
Other *Salix*	T	T	A	I	I	Y	3.02	0.27	1.62	0.42	7.4	1.15	352	82	88.7	2.4

Amino acid differences between the LSU sequences of *Salix* Rubisco and the corresponding Rubisco kinetic parameters, describing the Michaelis–Menten constants for CO_2 (K_c) and O_2 (K_o), the maximum rate of carboxylation k^c_{cat} and oxygenation (k^o_{cat}), and the specificity factor ($S_{c/o}$). Only those residues which differ between the 11 species of *Salix* species are shown. Kinetic constants for *S. triandra*, R13, and *S. exigua* are the means of two biological replications, while those for the remaining Rubisco isolates – which were considered to be identical – were combined, giving (eight biological replicates). Values of k^o_{cat} were calculated using the equation $S_{c/o} = (k^c_{cat}/K_c)/(k^o_{cat}/K_o)$. Two values for the LSD at the 5% confidence interval are shown; one for comparison between the top three genotypes ($n = 2$) and one for comparison between the value at the bottom ($n = 8$) and those above. In all cases, the degrees of freedom for calculation of LSD was 10. [Correction added on 15 December 2014, after first online publication: The first 4 headings of the 5 categories of parameter under Rubisco kinetic constants were previously incorrect and these have now been replaced.]

with $P < 0.05$ and $P < 0.01$. The one-way analysis of variance (ANOVA) treatments (SigmaPlot 12.0) of Figure 4 state mean values and the standard error of difference (SED) between the means, with 20–22 degrees of freedom depending on the response variable. The ANOVA of Table 4 is similar to that of Figure 4, except values for the least significant difference (LSD) at the 5% confidence interval are given, and the associated degrees of freedom stated in the legend. Other figures show specific comparisons between parameter sets, indicating mean values ± standard errors ($n = 3$) together with the derived correlation coefficient, *r*.

Results

Measuring leaf photosynthesis

In both years, *S. daphnoides* and *S. exigua* represented the upper and *S. dasyclados* the lower extremes of *A*/*Ci* performance, respectively (Fig. 1). For clarity, the dependence of *A* on intercellular CO_2 concentration (*Ci*) is shown for four (rather than all 11) of the genotypes, chosen to illustrate the range of observed responses. Values of V_{cmax} and *J* were determined (Fig. 2) which – when substituted into the equations of Farquhar and von Caemmerer describing RuBP carboxylation- and regeneration-limited CO_2 assimilation (von Caemmerer 2000) – described curves which faithfully followed the observed *A*/*Ci* data points for each genotype (Fig. 1, solid lines). Collectively, the values of V_{cmax} and *J* for all genotypes from both years could be described by a linear relationship, with a gradient (J/V_{cmax}) of approximately 2. The distribution of values differed between the 2 years – showing a broader range of values in 2008 (□) than 2009 (◇). Even so, the four genotypes with the highest values, and the three genotypes with the lowest values were the same in each year, although data points from 2008 appeared to have marginally higher rates of electron transport for any given V_{cmax} than those of 2009, the mean values for J/V_{cmax} being 2.24 ± 0.30 and 2.05 ± 0.10, respectively.

Diverse responses to light intensity were also found. The light dependence of photosynthesis was faithfully described for all genotypes in both years by a series of hyperbolic functions (eq. 1, Material and Methods), from which values for the light-saturated rates of CO_2 assimilation (A_{maxQ}), the photosynthetically active radiation required to achieve half these rates (effectively the K_M for photon flux density, $Q_{½}$), and the light compensation point (Γ_Q) could be derived. A linear relationship was found between light-saturated

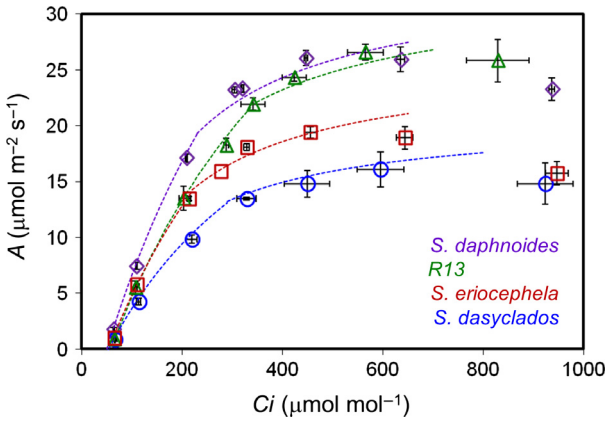

Figure 1. Dependence of leaf CO_2 assimilation (A) on intercellular CO_2 concentration (*Ci*). Data from a representative selection of genotypes in 2009. Light intensity 1250 μmol PAR m^{-2} sec^{-1}; leaf temperature 25 ± 1°C; relative humidity 60%. Each measurement was the mean of three biological replications, for which mean values and standard errors are indicated. The dotted lines show the modeled curves, based on the average values of V_{cmax} and *J* for each genotype.

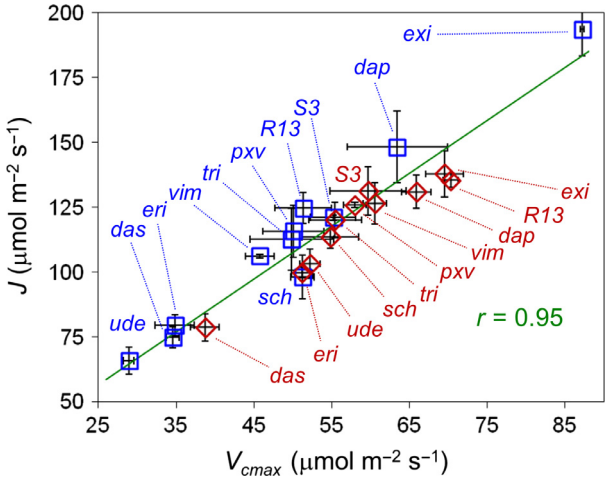

Figure 2. Correlation between maximum rates of Rubsico-limited and electron-transport-limited photosynthesis (V_{cmax} and *J*, respectively). Values derived by an iterative procedure (Sharkey et al. 2007) using *A*/*Ci* data for each genotype from both years. During this procedure, V_{cmax} and *J* were varied to minimize the deviation of the modeled curve from the observed data points. The resulting values were then normalized to 25°C. Each measurement was the mean of three biological replications, for which mean values and standard errors are indicated: 2008 (blue) and 2009 (red).

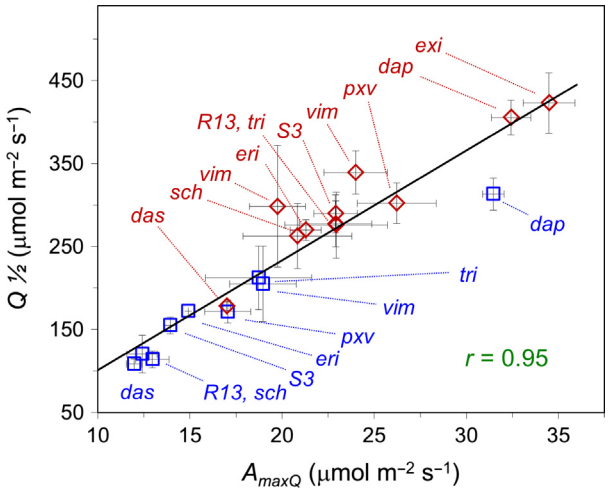

Figure 3. Correlation between rates of CO_2 assimilation at light saturation (A_{maxQ}) and the irradiance required to achieve 50% of these rates ($Q_{½}$). Data derived from a study of the light dependence of photosynthesis in both years, with chamber conditions set to 385 μmol CO_2 mol^{-1}, 25°C, 60% relative humidity. 2008 (blue) and 2009 (red). Each measurement was the mean of three biological replications, for which mean values and standard errors are indicated.

A_{maxQ} and $Q_{½}$ among the chosen genotypes from both years (Fig. 3). Values for the same genotype between years showed greater variation that the *A*/*Ci* data, although the relative positions of the extremes of performance were similar.

Identifying relationships across a wider range of parameters

In addition to those above, a selection of additional biochemical, physiological, and yield-related parameters were measured in the first year of growth (2008). Those relating to gross leaf morphology (size and specific leaf area) and photosynthetic performance were made in early/mid-Summer (late June) in parallel with leaf sampling for constituent analysis. Multiple pair-wise correlations between all the measured and derived parameters identified/confirmed likely positive and negative relationships (at $P > 99\%$ and $P > 95\%$) between many of these. The pattern and significance of the derived correlations were virtually identical when either the ungrouped (not shown) or the grouped (mean) data for each genotype were treated in this way (Table 2). In particular, a consistent, positive correlation was evident between total leaf protein and all parameters relating to leaf level photosynthesis (Table 2, col 19) and especially between leaf Rubisco and both light and CO_2 saturated photosynthesis (Table 2, col 10 and also row K). The same was also indicated for total leaf chlorophyll. In contrast, DM and leaf starch both showed strong negative correlations with maximum leaf photosynthetic rate, both at ambient (A_{amb}) and saturating CO_2 (A_{max}) or saturating light (A_{maxQ}). However, as elaborated below, when the total leaf area per plant was estimated from leaf number and size data, and whole plant photosynthetic capacity estimated by combining this with the ambient rates per unit leaf area (as an estimate of the whole plant photosynthetic rate [ΣA_{amb}]), then a significant positive correlation between ΣA_{amb} and both DM and starch was indicated (Table 2). Surprisingly, although total leaf area (m^2/plant) was positively correlated to DM, leaf starch, and leaf size (cm^2/leaf) and negatively with all parameters relating to leaf level photosynthesis, and specific leaf area (SLA, cm^2/g DM) showed little correlation to any of the measured parameters, except light compensation point (Γ_Q).

A similar collection of paired correlations was constructed using data from the second season (2009). As described previously, the pattern and significance of the derived correlations were virtually identical when either the ungrouped (not shown) or grouped (mean) data for each genotype were analyzed (Table 3). In this season, emphasis was placed on detailed measurement of shoot biomass and total leaf area from mid-June ("early Summer") and again from early August ("mid/late Summer"), together with leaf photosynthesis.

In early Summer (Table 3, col 14 and 15) total plant leaf area and whole plant photosynthetic potential (ΣA_{amb}) showed strong positive correlation to final yield (shoot DM, shoot volume, and root DM – rows A, B, and C) and equally strong negative correlations to a variety of photosynthetic

characteristics expressed per unit leaf area (A_{amb}, A_{max}, A_{maxQ}, V_{cmax} Table 3, col 14 and 15). In mid/late Summer, the negative correlations between total plant leaf area and the same leaf level photosynthetic parameters were even more pronounced (Table 3, col 17) although photosynthetic potential – expressed on a whole plant basis – showed a weaker correlation to final yield (Table 3, col 20).

Identifying relationships between specific parameters

Mean (and SED) values for some of the parameter sets obtained in 2008 and 2009 and ranked according to magnitude are shown (Fig. 4) to illustrate the range and significance of a collection of the measured values. Although there are clear differences between the extremes of performance, the intermediate genotypes showed some degree of overlap. However, when the correlation between pairs of data sets was examined, likely relationships emerged. Some noteworthy examples are elaborated here.

Biomass yield and photosynthetic rate

Biomass yield and photosynthetic rate under ambient CO_2 and near-saturating light in the early Summer (A_{amb}) showed a weak, negative correlation (Table 3, row A, columns 5 and 20). However, graphical illustration of this relationship (using the early Summer yield data) highlighted a subset of genotypes which demonstrated a highly significant, positive correlation (Fig. 5A, red vs. black line). When the correlation between leaf area per plant and yield was examined (Fig. 5B), a significant correlation to which all species broadly conformed was found. An even more significant correlation was observed when both leaf area per plant and assimilation rate per unit leaf area were integrated (Fig. 5C), which again was a correlation to which all genotypes conformed. Thus, both leaf area per plant and assimilatory capacity per unit leaf area appear to make significant contributions to biomass. V_{cmax} and leaf area per plant were inversely correlated (Fig. 6). Since V_{cmax} is a function of the leaf content of Rubisco, we also compared leaf area and leaf Rubisco concentration, and found that they were most strongly (negatively) correlated in the mid/late Summer – as would be expected since (in 2009) the samples for Rubisco analysis had been taken over this period (Table 3, column 18).

Leaf starch content and maximum photosynthetic rate

Leaf starch content – measured in leaf samples taken in the mid-afternoon in early Summer (3–4 h after midday) – showed a strong negative correlation with parallel measurements of maximum leaf photosynthetic rate at saturating CO_2 (A_{max}) (Fig. 7) as well as with numerous other photosynthetic processes (Table 2, col 16 and row Q).

The correlation between common data sets measured in 2008 and 2009, while not identical, nonetheless indicate similar relative rankings between the diverse genotypes between successive years (Fig. S2).

Probing Rubisco diversity among the willow genotypes

Rubisco was sampled from collections of young, fully expanded leaves of each genotype in the late Spring. These samples provided material for subsequent extraction and/or purification of Rubisco, for determination of the relative specificity for CO_2 and O_2 ($S_{c/o}$) as well as the rate constants for carboxylase and oxygenase activities (k^c_{cat} k^o_{cat}, respectively), and the Michaelis constants for CO_2 and O_2 (K_c and K_o, respectively). In parallel, DNA was extracted and the LSU gene sequences determined. The GenBank accession numbers for these sequences are given in Table 1, and the integrated data in Table 4, with additional kinetic data given in Table S1. Significant differences were identified between the genotypes with respect to (k^c_{cat}), (k^o_{cat}), and K_c (Table 4).

For nine of the genotypes, the LSU gene sequences were identical. Compared to these, the *S. triandra* sequence contained three different codons, representing amino acid substitutions T9A, T142P, and A230T, while *S. exigua* contained three distinct residue substitutions, these being, I255V, I309M, and Y363F together with an alternative substitution, T142V (Table 4).

A comparison of the maximum carboxylation rate of Rubisco (V_{cmax}) for each willow species, as deduced from gas exchange measurements, with the corresponding parameters deduced from direct measurement of the leaf Rubisco concentration and the rate constant for carboxylation is shown in Figure S4. This reveals that the activity of Rubisco during the photosynthesis measurements was considerably lower than would be expected based on the measured Rubisco content and catalytic characteristics.

Discussion

Leaf photosynthesis

The mean rates of photosynthesis at ambient CO_2 reported here for *S. viminalis* "Bowles hybrid" (19.5 ± 1.0 [SD, $n = 3$]) and *S. dasyclados* (13.7 ± 0.1 [SD, $n = 3$]) are very similar to those reported by Patton and Jones (1989) (i.e., 17.2 ± 2.3 and 13.9 ± 1.3, respectively). The values of V_{cmax} and J (Fig. 2) derived from the *A/Ci* analyses (Fig. 1) define the maximum rates of Rubisco-dependent (A_c) and

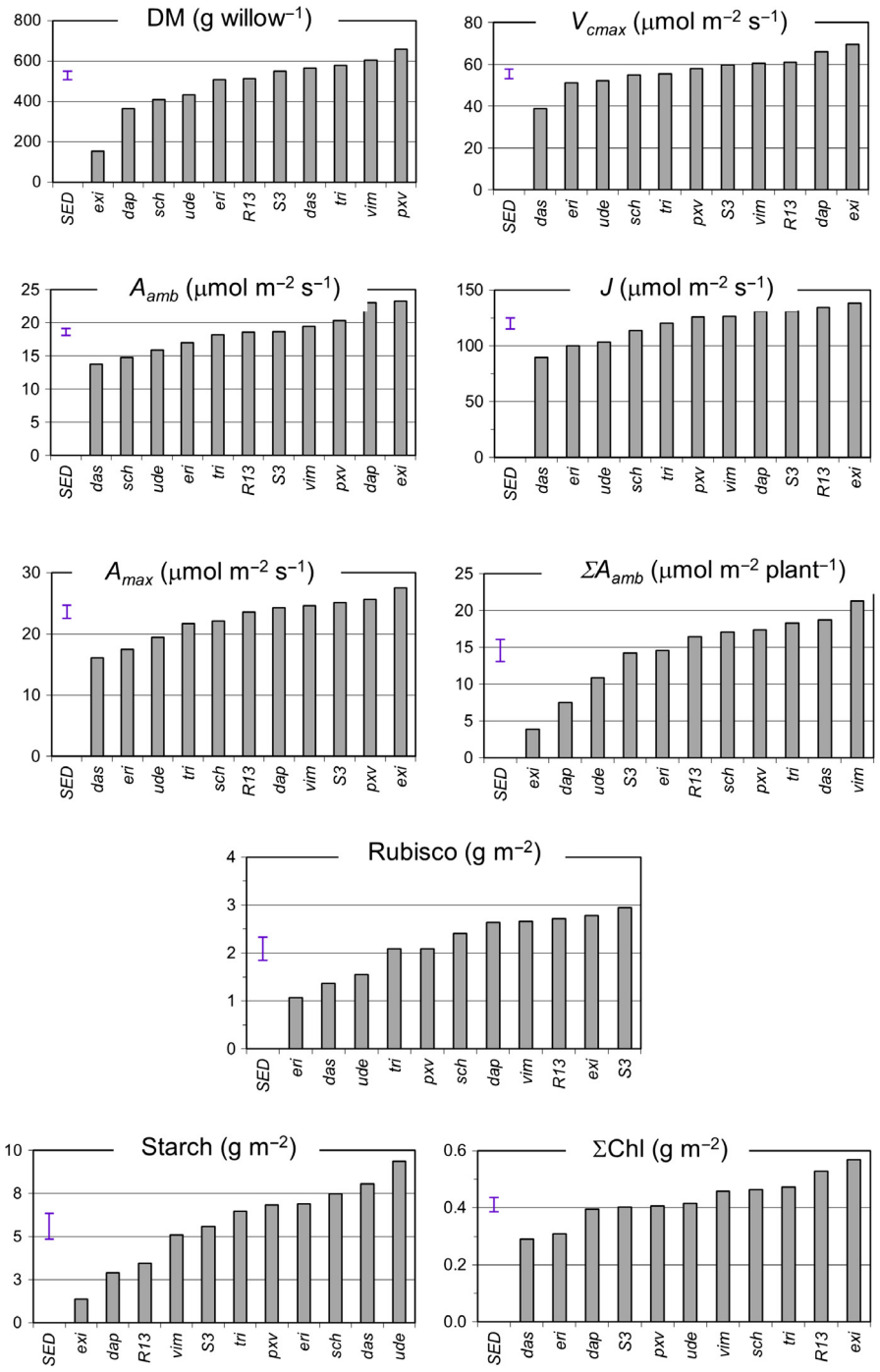

Figure 4. Means and SED values for an assortment of genotype properties. The data were from the 2009 experiment, except for starch and total chlorophyll (Σ*Chl*) which were from 2008. Photosynthetic capacity on a whole plant basis (ΣA_{amb}) was measured in early Summer (end June/early July). Each measurement was the mean of three biological replications. Each data set was analyzed for statistical significance using a one-way analysis of variance (SigmaPlot 12.0) from which the mean values and standard error of difference (SED) between the means (with 20–22 degrees of freedom depending on the response variable) are shown.

RuBP-regeneration-dependent (A_j) CO_2 assimilation, respectively, as well as the initial gradient of the *A/Ci* relationship and the maximum attainable assimilation rates. The ratio, J/V_{cmax} (at 25°C) typically ranges between 1.5 and 2.0 (von Caemmerer 2000) which are similar to the values determined here (2.0–2.5). In an analysis across a range of woody plant

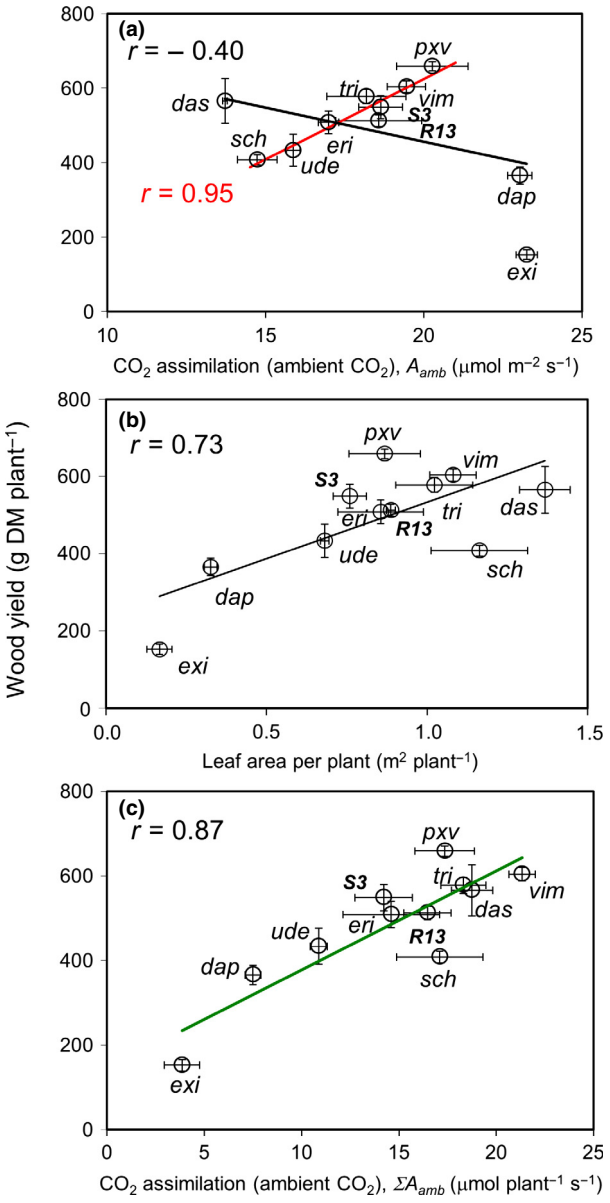

Figure 5. (A) Correlation between yield and photosynthesis at ambient (385 μmol mol^{-1}) CO_2, 25°C, 60% relative humidity. The overall regression line is shown in black, while that shown in red applies to the cluster of points in the center. Values shown are means ± standard error (n = 3). (B) Correlation between yield and whole plant leaf area. (C) Correlation between yield and whole plant photosynthesis (calculated as: μmol CO_2 fixed m^{-2} sec^{-1} × leaf m^2 plant^{-1}). Coefficients derived from Pearson product–moment correlations, as implemented by SigmaPlot 12.0, are shown. All data were from the 2009 experiment.

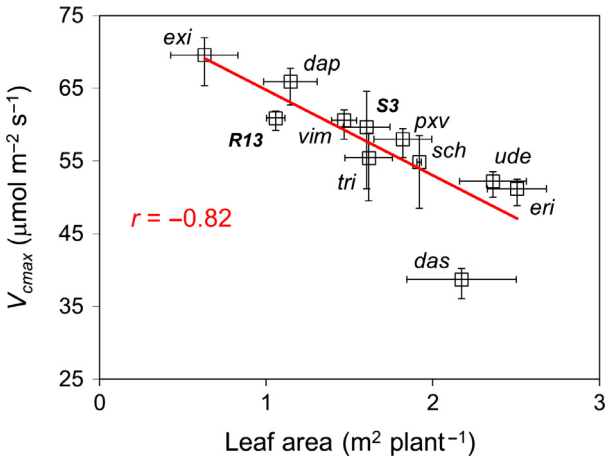

Figure 6. Correlation between V_{cmax} and leaf area per plant. Values shown are means ± standard error for 2009 data set (n = 3).

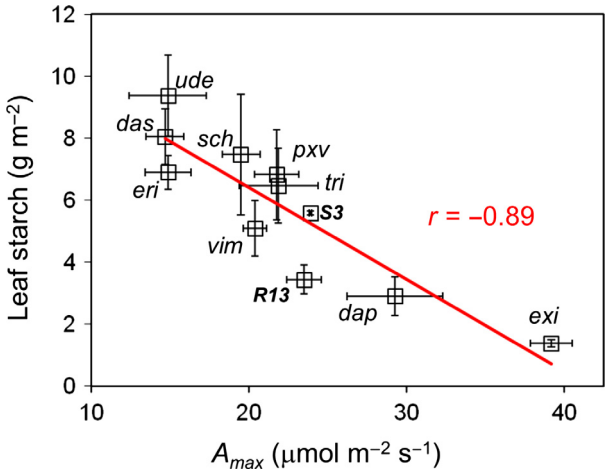

Figure 7. Correlation between photosynthesis at CO_2 saturation (A_{max}) and leaf starch, 3–4 h after midday. Values shown are means ± standard error from 2008 (n = 3).

species, Manter and Kerrigan (2004) also found a linear correlation between J and V_{cmax} analogous to that of Figure 2, with a mean ratio (J/V_{cmax}) of 2.5. By contrast, Robinson et al. (2004) measured ratios of 4.5 and 5.2 for high- and low-yielding willow species, respectively. Our data are consistent with a narrow range of J/V_{cmax} ratios among the willows investigated, irrespective of yield capacity. The absolute amounts of the components which determine J and V_{cmax} will also impact on the observed rates of photosynthesis. Thus, *S. exigua* and *S. daphnoides*, which in both years showed the highest rates of photosynthesis at both ambient and saturating CO_2 (Figs. 1, 4) also had the highest V_{cmax} and J, while *S. dasyclados*, which had among the lowest rates in both years, also had the lowest V_{cmax} and J (Figs. 1, 2, and 4). These observations were complemented by the total leaf protein, chlorophyll (Table 2), and Rubisco (Tables 2, 3) measurements, all of which correlated positively with leaf photosynthetic performance. The process of parameter optimization to obtain the best values of V_{cmax} and J (Sharkey

et al. 2007) also generated complementary values for light-independent respiration (R_d) and mesophyll conductance (*gm*). However, no significant correlations were evident using these values (not shown). In addition, the *Ci* at which the RuBP carboxylation limited rate of CO_2 assimilation is identical to the RuBP regeneration limited rate of CO_2 assimilation (the "tipping point") was generally in the vicinity of the observed *Ci* when the leaves were in normal air, and showed no consistent trend between the genotypes (not shown).

Considerable diversity was also apparent in the light dependence of photosynthesis among the willow genotypes; the estimated light-saturated rates of photosynthesis (at ambient CO_2) differing by up to 2.5-fold between the extremes of performance (Fig. 3). The genotypes with the highest photosynthetic rates at both ambient and saturating CO_2 also possessed the highest rates at light saturation and the highest irradiances to attain half this value.

Identifying relationships between parameters at specific periods

One important observation is that photosynthetic rate – either at ambient or saturating CO_2 – together with many of the underlying processes contributing to leaf photosynthetic performance (Rubisco, total protein, chlorophyll) were negatively correlated to yield. In contrast, total leaf area per plant was positively correlated to yield, particularly in the early Summer period (Tables 2, 3, Fig. 5A). However, yield is a function of both total leaf area and leaf photosynthetic rate (per unit leaf area). This is evident from Figure 5 where the rate of assimilation of eight of the species was very significantly correlated to yield (Fig. 5A). However, the total leaf area per plant for all genotypes was also significantly correlated to yield (Fig. 5B, $P < 0.01$). When these two components were integrated, the resulting whole plant photosynthetic capacity was also very significantly correlated to yield ($P < 0.001$). Yield and the corresponding parameters from mid/late Summer were less significantly correlated. Since the average factor by which leaf area increased over this period was 2.6 ± 0.5 (SD), the poorer correlation later in the season may have been due to leaf capacity being in increasing excess over available radiation. In other words, a slowly diminishing amount of solar radiation (since the solar angle and day length both diminish after June 21) was shared across an increasing total plant leaf area.

The relationship between starch, soluble carbohydrate, yield, and photosynthesis

The immediate products of photosynthesis – soluble carbohydrate and starch – measured in the late afternoon, showed a weak, positive correlation to yield, a stronger positive correlation to total leaf area per plant, and (particularly starch) a strong negative correlation to many components of the photosynthetic process (Table 2, columns 15 and 16). The latter observation prompts the question as to whether accumulation of leaf starch over this period, triggers processes which diminish photosynthetic rate. However, since starch is insoluble, the effects of starch accumulation may need to be relayed by a soluble factor whose concentration is responsive to starch. The obvious candidate for this would be a soluble sugar, which may explain the similar (albeit weaker) negative correlations between soluble carbohydrate and an assortment of photosynthetic components. More detail on the correlation between high starch content in leaves and low assimilation rate can be found elsewhere (Paul and Foyer 2001), although a strong negative correlation between net photosynthetic rate and starch concentration, independent of carbohydrate concentration, has been attributed to an increase in mesophyll (liquid phase) CO_2 diffusion resistance, suggesting that starch accumulation may reduce net photosynthetic rate by impeding intracellular CO_2 transport (Nafziger and Koller 1976). A key role for starch in the integration of plant growth has been reported (Selbig et al., 2009) although in that study (using Arabidopsis) it was found to correlate negatively with biomass, while the current study reports a positive correlation with biomass – of both shoot and leaf (Table 2).

A question of scale

The barely significant, negative, correlations between yield and many indicators of leaf photosynthetic performance, expressed per m^2 of leaf (A_{amb}, A_{max}, V_{cmax}, J, $Q_{½}$, A_{maxQ}, Γ_Q, and Rubisco; Table 3, rows A, B, and C) were all seen in fact to be significantly ($P > 0.05$) and positively correlated (with yield) when (like leaf photosynthesis itself, Fig. 5) these parameters were expressed on a whole plant basis (Fig. S3). The same was also true of the corresponding parameters of Table 2 (not shown). Evidently, the nature of an observed correlation depends on the way (or units) in which the parameters in question are expressed. That being so, in future it may be informative to relate photosynthetic parameters determined for much larger populations of plants obtained by measurements made over a similarly large area (e.g., by application of Eddy Covariance techniques) to biomass yields per hectare.

Assumptions, limitations, and shortcomings

The study of pot-grown material under glass was not intended to be a realistic substitute for field-grown material. However, in an attempt to ensure healthy, nutritionally replete, and otherwise unstressed plants in the same soil substrate at identical developmental stages, this approach was considered

to be justified. It is unlikely that differences in the mass of the planted cuttings were responsible for the differences in willow growth recorded here (Hangs et al., 2011), neither are the differences in leaf level photosynthesis likely to be due to N availability – as identical growth media were used throughout and as fertilization has been shown to have little effect on leaf photosynthesis (Merilo et al. 2006). However, the absence of lateral shading – which would normally be present in dense plantations – may have led to unrealistic growth rates (and possibly other characteristics). Additional problems associated with restriction of root development may also have been present –and would undoubtedly have become more severe if the experiment had continued for more than a single season.

Furthermore, the photosynthetic performance of the youngest fully expanded leaves, measured under ideal, light-saturated conditions, together with a careful assessment of leaf area per plant, have been used to estimate the actual whole plant photosynthetic capacity. While this is no doubt on oversimplification, we did not have sufficient resources to conduct a more thorough investigation which, for example, might have investigated gradients of photosynthetic performance in leaves at different positions along the axis of the main stem and/or could have incorporated more stages in the season. Even so, we believe that the comparisons of estimated performance between genotypes attempted in this study are of value.

The extent of yearly variation between the photosynthetic parameters measured was surprising, although the correlation for yield remained strong (Fig. S1). Such differences are presumably due to the variation in summer irradiance and temperature between years.

Rubisco diversity among willow genotypes

Three of the six polymorphic LSU residues identified in Table 4 – namely 142, 255, and 309 – are positions which are among those most frequently found to be positively selected in evolutionary adaptation of the LSU (Kapralov and Filatov 2007). Residue identity at position 309 (typically methionine or isoleucine) correlates with kinetic differences between C_3 and C_4 forms of *Flaveria*, respectively (Kapralov et al. 2011). In the context of the *Flaveria* LSU sequence, isoleucine 309 has been shown to act as a catalytic switch that increases the Rubisco carboxylation rate (k^c_{cat}). An analogous situation is reported here between *S. triandra* (residue 309 = isoleucine) and *S. exigua* (residue 309 = methionine). In fact, all the LSU sequences determined, except that of *S. exigua*, had isoleucine at this position – and correspondingly had (4–29%) higher values for (k^c_{cat}) (Whitney et al., 2011) than *S. exigua*. But the extent of this difference and the relative magnitude of the other kinetic parameters differed. This is presumably due to the effects of the other LSU residue changes which were observed. It is puzzling that R13 – whose LSU sequence was identical to that of the willow "consensus" sequence – was found to have distinct (k^o_{cat}) and K_c values (Table 4). This is presumably due to diverse properties of the accompanying nuclear-encoded small subunits, of which there are likely to be multiple, distinct, copies in each genotype, and which have been shown to differentially influence the kinetic properties of Rubisco (Ishikawa et al. 2011).

Making use of the modest differences in (k^c_{cat}), (k^o_{cat}), and K_c (Table 4) between the polymorphic willow LSUs, is beyond the scope of the current study, although these values generate distinct modeled *A/Ci* curves, assuming the leaves contained equal amounts of Rubisco and equal amounts of the components of RuBP regeneration, per unit leaf area (Fig. S2). All else equal, such differences could have a significant impact on performance over a range of *Ci* values, especially at lower *Ci*. Stomatal closure induced by water deficit will cause *Ci* to decline, as photosynthesis proceeds (Farquhar and Sharkey 1982). Under these conditions, species – like *S. triandra* – whose Rubisco can support higher rates of CO_2 assimilation (up to twofold more than R13 at *Ci* = 200 μmol mol^{-1}) would have a clear advantage. However, the modeled behavior was not reflected in the observed *A/Ci* curves or in the derived values for V_{cmax} and *J* (Figs. 1, 2), most likely owing to the actual leaf concentrations of Rubisco – which were greater in R13 and *S. exigua* than in many of the other genotypes (Fig. 4).

Mismatch between Rubisco activity and abundance

The species-specific, maximum carboxylation capacity of Rubisco (V_{cmax}) predicted from *A/Ci* analyses (e.g., Figs. 2, 4), may underestimate the actual V_{cmax}, as deduced from direct measurement of species-specific Rubisco abundance and catalytic capacity. Figure S4 presents a comparison between these alternative measures of V_{cmax} from 2009 (although the same was also apparent in 2008). One explanation for such a mismatch would be that the *A/Ci* measurements were not made with adequate (near saturating) light. This is very unlikely, since the mean photon flux density ($Q_{½}$) at which half the predicted light-saturated rate of photosynthesis was evident – was approximately 250 μmol photons m^{-2} sec^{-1} (Fig. 3), while the measuring intensity was 5× higher than this, and represented a similar level of exposure as that on a cloudless day under glass. A more likely explanation would be either that Rubisco was present in excess of requirement and that the excess catalytic capacity had been downregulated, or else that limitations existed in the Rubisco regulatory mechanism, preventing full expression of the available Rubisco activity. This possibility may be worth pursuing in future.

Concluding Remarks

This study assessed photosynthetic capacity and contributory processes in a broad range of genotypes to determine whether sufficient natural variation relevant to yield existed to warrant the initiation of genetic improvement strategies targeting the underlying genes. Significant differences in photosynthetic parameters and yield between the genotypes studied were identified and imply strong genotypic control of all these properties. A variety of parameters – expected to positively impact upon photosynthetic performance – were measured for each genotype and were collectively found to correlate positively with photosynthesis. Although a positive correlation between photosynthetic rate and biomass was only described by a subset of genotypes, at a specific period in the growing season (Fig. 5A), when leaf area was taken into account (Fig. 5B) and photosynthetic rate expressed on a whole plant basis (Fig. 5C), then it emerged as being positively correlated to yield: strongly during early Summer, but also later on, albeit less significantly (Table 3). It also emerged that when a variety of other performance-related photosynthetic parameters were expressed on a per plant basis (taking into account the leaf area per plant), they were also found to be positively correlated with yield (Fig. S3). This indicates that plant leaf area has been a more significant adaptive criterion for controlling growth among *Salix* genotypes, than the mechanistic capacity in a given leaf area. The kinetic properties of Rubisco make a significant contribution to V_{cmax} and J (the former through (k^c_{cat}), K_c, and K_o, than latter through specificity factor). These properties were shown to be distinct between certain willow genotypes, consistent with differences in their LSU gene sequences, also identified in this work. Hence, distinct, heritable traits relating specifically to Rubisco (and therefore photosynthetic) performance have been identified, consistent with our overall objectives. *Salix* varieties with higher photosynthetic rates per unit leaf area, relative to whole plant leaf area, have been shown to result in greater yields (Bouman and Sylliboy, 2012). Thus, in common with other commercially important plant species, improvements in photosynthetic efficiency in *Salix* has significant potential for yield improvement (Long et al. 2006).

Acknowledgments

We acknowledge the advice of Elina Vapaavuori (of the Finnish Forest Research Institute) during our initial attempts to extract protein (particularly active Rubisco) from our leaf material. We also thank William Macalpine for assisting in the identification of willow genotypes in the field; March Castle and Tim Barraclough for helping with the harvest shoot volume measurements of the 2009 experiment; Jérémy Guinard for assisting with the gas exchange measurements in 2008; and the glasshouse staff at Rothamsted Research for technical support throughout. P. J. A., P. J. M., and M. A. J. P. are supported by the UK Biotechnological and Biological Sciences Research Council (BBSRC) 20:20 Wheat® Institute Strategic Program (BBSRC BB/J/00426X/1) and BBSRC BB/I002545/1 and BB/I017372/1, and A. K. and I. F. S. are supported by the BBSRC Cropping Carbon Institute Strategic Program (BB/J004278/1). Rothamsted Research is an Institute supported by the BBSRC.

Conflict of Interest

None declared.

References

Bouman, O. T., and J. Sylliboy. 2012. Biomass allocation and photosynthetic capacity of willow (*Salix* spp.) bio-energy varieties. Forstarchiv 83:139–143.

van Caemmerer, S. 2000. P. 45 *in* Biochemical models of leaf photosynthesis. Chapter 3 – modelling C_3 photosynthesis, CSIRO Publishing, Canberra, Australia.

Cannell, M. G. R., R. Milne, L. J. Sheppard, and M. H. Unsworth. 1987. Radiation interception and productivity of willow. J. Appl. Ecol. 24:261–278.

Christersson, L. 1987. Biomass production by irrigated and fertilized *Salix* clones. Biomass 12:83–95.

Ericsson, T., L. Rytter, and E. Vapaavuouri. 1996. Physiology of carbon allocation in trees. Biomass Bioenergy 11:115–127.

Farquhar, G. D., and T. D. Sharkey. 1982. Stomatal conductance and photosynthesis. Annu. Rev. Plant Phys. Plant Mol. Biol. 33:317–345.

Galmés, J., J. Flexas, A. J. Keys, J. Cifre, R. A. C. Mitchell, P. J. Madgwick, et al. 2005. Rubisco specificity factor tends to be larger in plant species from drier habitats and in species with persistent leaves. Plant Cell Environ. 28:571–579.

Hangs R. D., Schoenau J. J., Van Rees K. C. J., Steppuhn, H. 2011. Examining the salt tolerance of willow (Salix spp.) bioenergy species for use on salt-affected agricultural lands. Can. J. Plant Sci. 91:509–517.

Hanley, S. J., and A. Karp. 2013. Genetic strategies for dissecting complex traits in biomass willows (*Salix* spp.). Tree Physiol. doi: 10.1093/treephys/tpt089

Hansen, J., and I. Møller. 1975. Percolation of starch and soluble carbohydrates from plant tissue for quantitative determination with anthrone. Anal. Biochem. 68:87–94.

Ishikawa, C., T. Hatanaka, S. Misoo, C. Miyake, and H. Fukayama. 2011. Functional incorporation of sorghum small subunit increases the catalytic turnover rate of Rubisco in transgenic rice. Plant Physiol. 156:1603–1611.

Kapralov, M. V., and D. A. Filatov. 2007. Widespread positive selection in the photosynthetic Rubisco enzyme. BMC Evol. Biol. 7:73.

Kapralov, M. V., D. S. Kubien, I. Andersson, and D. A. Filatov. 2011. Changes in rubisco kinetics during the evolution of C4 photosynthesis in flaveria (Asteraceae) are associated with positive selection on genes encoding the enzyme. Mol. Biol. Evol. 28:1491–1503.

Karp, A., and I. Shield. 2008. Bioenergy from plants and the sustainable yield challenge. New Phytol. 179:15–32.

Karp, A., S. J. Hanley, S. O. Trybush, W. Macalpine, M. Pei, and I. Shield. 2011. Genetic improvement of Willow for bioenergy and biofuels. J. Integr. Plant Biol. 53:151–165.

Liu, M. Z., G. M. Jiang, Y. G. Li, L. M. Gao, S. L. Niu, H. X. Cui, et al. 2003. Gas exchange, photochemical efficiency, and leaf water potential in three *Salix* species. Photosynthetica 41:393–398.

Long, S. P., X. G. Zhou, S. L. Naidu, and D. R. Ort. 2006. Can improvement in photosynthesis increase crop yields? Plant Cell Environ. 29:315–330.

Manter, D. K., and J. Kerrigan. 2004. A/Ci curve analysis across a range of woody plant species: influence of regression analysis parameters and mesophyll conductance. J. Exp. Bot. 55:2581–2588.

Merilo, E., K. Heinsoo, and O. Kull. 2006. Leaf photosynthetic properties in a willow (*Salix viminalis* and *Salix dasyclados*) plantation in response to fertilization. Eur. J. Forest Res. 125:93–100.

Miller, S. A. 2010. Minimizing land use and nitrogen intensity of bioenergy. Environ. Sci. Technol. 44:3932–3939.

Nafziger, E. D., and H. R. Koller. 1976. Influence of leaf starch concentration on CO_2 assimilation in soybean. Plant Physiol. 57:560–563.

Neergaard, A. D., J. R. Porter, and A. Gorissen. 2002. Distribution of assimilated carbon in plants and rhizosphere soil of basket willow (*Salix viminalis* L.). Plant Soil 245:307–314.

Parry, M. A. J., P. J. Madgwick, J. F. C. Carvalho, and P. J. Andralojc. 2007. Prospects for increasing photosynthesis by overcoming the limitations of Rubisco. J. Agric. Sci. 145:31–43.

Patton, L., and M. B. Jones. 1989. Some relationships between leaf anatomy and photosynthetic characteristics of willows. New Phytol. 111:657–661.

Paul, M. J., and C. H. Foyer. 2001. Sink regulation of photosynthesis. J. Exp. Bot. 52:1383–1400.

Robinson, K. M., A. Karp, and G. Taylor. 2004. Defining leaf traits linked to yield in short-rotation coppice *Salix*. Biomass Bioenergy 26:417–431.

Selbig, J., A. R. Fernie, T. Altmann, and M. Stitt. 2009. Starch as a major integrator in the regulation of plant growth. Proc. Natl Acad. Sci. USA 106:10348–10353.

Sharkey, T. D., C. J. Bernacchi, G. D. Farquhar, and E. L. Singsaas. 2007. Fitting photosynthetic carbon dioxide response curves for C3 leaves. Plant Cell Environ. 30:1035–1040.

Taylor, G., K. P. Beckett, K. M. Robinson, K. Stiles, and A. M. Rae. 2001. Identifying QTL for yield in biomass poplar. Aspects Appl. Biol. 65 (Biomass and energy crops II):173–182.

Tharakan, P. J., T. A. Volk, C. A. Nowak, and L. P. Abrahamson. 2005. Morphological traits of 30 willow clones and their relationship to biomass production. Can. J. For. Res. 35:421–431.

Trybush, S., S. Jahodova, W. Macalpine, and A. Karp. 2008. Genetic studies of a germplasm resource reveal new insights into relationships among *Salix* subgenera, sections and species. BioEnergy Res. 1:67–79.

Whitney, S. M., R. E. Sharwood, D. Orr, S. J. White, H. Alonso, and J. Galmés. 2011. Isoleucine 309 acts as a C_4 catalytic switch that increases ribulose-1,5-bisphosphate carboxylase/oxygenase (rubisco) carboxylation rate in *Flaveria*. Proc. Natl Acad. Sci. USA 108:14688–14693.

Wintermans, J. F. G. H., and A. De Mots. 1965. Spectrophotometric characteristics of chlorophylls a and b and their phaeophytins in ethanol. Biochim. Biophys. Acta 109:448–453.

Yokota, A., and D. T. Canvin. 1985. Ribulose bisphosphate carboxylase/oxygenase content determined with [^{14}C] carboxypentitol bisphosphate in plants and algae. Plant Physiol. 77:735–739.

Supporting Information

Additional supporting information may be found in the online version of this article at the publisher's web-site.

Figure S1. The correlation between common data sets measured in 2008 and 2009. The nature of the data and the associated units are given in the title to each correlation.

Figure S2. Theoretical *A/Ci* curves, generated using the four distinct sets of kinetic parameters identified among the willow genotypes (shown in Table 4). To facilitate comparison, it was assumed that all leaves had the same Rubisco concentration (the mean value across both years, namely 29.7 ± 9.2 μmol active sites m^{-2}) and that the ratio of J to V_{cmax} was 2.16 (the mean ratio from data in Fig. 2).

Figure S3. Revealing significant positive correlations between components of CO_2 assimilation and willow biomass. (A) Mean leaf area in each willow species (error bars show SEM, n = 3); (B) (●) Correlation between wood yield (abscissa axes) and stated parameters (ordinate axes) expressed on a leaf area basis (leaf m^{-2}); (C) (○) As in (B) except stated parameters expressed on a whole plant basis ($plant^{-1}$) using data from (A). In (B) and (C) mean values (only) are shown. All data from early Summer (2009).

Figure S4. Species-specific carboxylase rate constants (k^c_{cat}) and Rubisco content (upper graph); and species-specific

V_{cmax} derived either by *A/Ci* analyses or by integration of rate constant (k^c_{cat}) and Rubisco content data. Each measurement was the mean of three biological replications, for which mean values and standard errors are indicated (nd, not determined). All data from 2009.

Table S1. Individual data sets used to generate the data of Table 4. Each line shows data obtained from a different leaf protein extract and plant. Each value was derived from a series of technical replications, each data set resulting from Rubisco assays at (a) six CO_2 concentrations, at each of four O_2 concentrations ((k^c_{cat}), (k^o_{cat}), K_c and K_o); or (b) five or six total (RuBP) consumption assays in an oxygen electrode ($S_{c/o}$), as described in Materials and Methods. Values are means ± standard deviation.

